**FINAL REPORT ON**

# Synthesis of oxide layer coated ZnO and $TiO_2$ nanoparticles and their application in dye sensitized solar cells

Sanctioned by UGC Vide F. No. 39-533/2010 (SR) dated 7.1.2011

For the period from 1.2.2011 to 31.1.2014

**Submitted to**

**University Grants Commission**
**Head office**
**New Delhi – 110 002**

**Submitted by**

**Dr. N. K. Verma**
**(Principal Investigator)**

**School of Physics and Materials Science**
**Thapar University**
**Patiala-147 004**
**Punjab, India**

**Annexure I**

## Project progress report

**Work done:**

Synthesis of $Tb_2O_3$ and $Eu_2O_3$ coated ZnO and $TiO_2$ nanoparticles by chemical synthesis route as well as the investigations of structural, morphological and optical properties of the synthesized nanoparticles has been done. These nanoparticles have been employed in DSSCs, and their photocurrent density-voltage (J-V) characteristics have been measured using source meter under simulated sun light.

**Synthesis and characterization of $Eu_2O_3$ coated ZnO nanoparticles and their application in dye sensitized solar cells**

Synthesis of $Eu_2O_3$ coated ZnO nanoparticles have been carried out by solvothermal synthesis route. For coating of $Eu_2O_3$; $EuCl_3$ and $NaBH_4$ are dissolved in ethanol and added drop-wise to dispersed solution of ZnO nanoparticles. This solution was treated in solvothermal cell at optimum temperature for required time.

For the fabrication of dye sensitized solar cells, the working electrodes for DSSCs were fabricated using synthesized nanoparticles by doctor blade technique. The electrodes were immersed in ethanolic solution of N719 dye for the adsorption of dye molecules on electrodes. The counter electrodes were prepared by spin coating of chloroplatinic acid hexahydrate on FTO glass. After assembling the dyed and the counter electrodes, a few drops of electrolyte, comprising of LiI, $I_2$, TBP, and TBAI, in acetonitrile, were injected in between the electrodes for complete fabrication of DSSC. The photocurrent-voltage (I-V) characteristics of the fabricated DSSC have been measured.

**Characterizations:** Following are some of the key results of the research work done.

**Structural analysis:** Figure 1 shows the XRD patterns of ZE0, ZE1, ZE2 and ZE3 samples. All the peaks in the XRD pattern of ZE0 are indexed to hexagonal structure with wurtzite phase, (JCPDS card No: 80-0075) with strong reflections from (101), (100) and (002) planes. The XRD pattern of ZE1 shows no peak related to $Eu_2O_3$ which shows $Eu_2O_3$ formed a very thin layer, which was too thin to be detected by XRD. In the XRD patterns of ZE2 and ZE3, the diffraction peak from cubic phase $Eu_2O_3$ is indexed to (222) (marked with * in figure 1),

as confirmed by the JCPDS card No: 74-1988, which demonstrates the existence of $Eu_2O_3$ on the surface of ZnO nanoparticles.

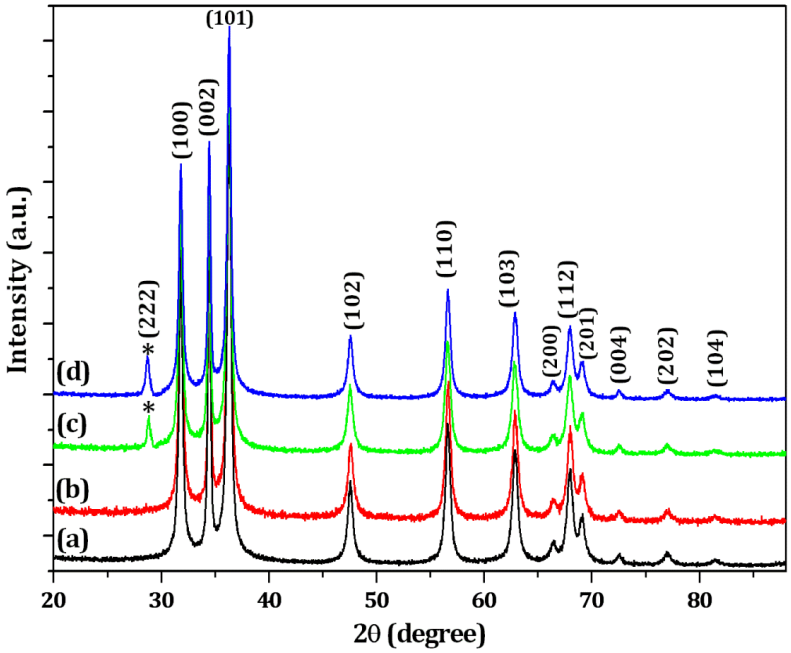


**Figure 1** X-ray diffractogram of (a) ZE0 (b) ZE1 (c) ZE2 and (d) ZE3 samples

**Compositional analysis**

Further to corroborate the XRD results, EDAX analysis has been carried out and shown in figure 2. For the sample, ZE0, the EDAX spectrum (figure 2(a)) shows distinct peaks of Zn and O, with atomic percentage 51.33 and 48.67, respectively, concluding stoichiometric formation of ZnO nanoparticles. The EDAX spectrum of the samples ZE1, ZE2 and ZE3 (figure 2(b), 2(c) and 2(d)) show the presence of Zn, O and Eu elements, indicating the presence of $Eu_2O_3$ coating on the ZnO nanoparticles, as observed in XRD patterns as well (figure 1). A systematic decrease in Zn content and a relative increase in the atomic percentage of Eu have been observed with the increasing concentration of $Eu_2O_3$ in the samples.

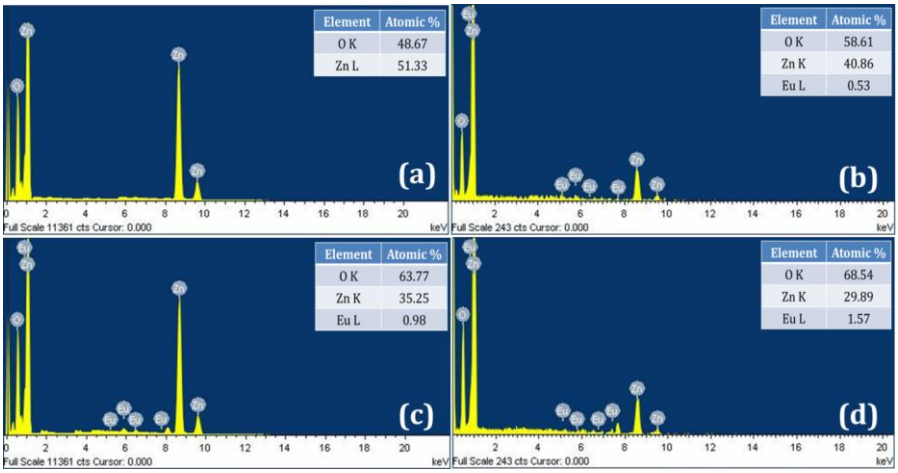


**Figure 2** EDAX spectrum of (a) ZE0 (b) ZE1 (c) ZE2 and (d) ZE3 samples

**Morphological analysis:** The presence of $Eu_2O_3$ on the surface of the ZnO nanoparticles has been established from TEM of ZE2 sample. TEM micrographs of ZE0 (figure 3(a)) and ZE2 (figure 3(b)) samples reveal their spherical nature with average particle size 9.4nm and 10.1nm, respectively. Figure 3(b) confirms the coating (shown by arrows in the inset) of $Eu_2O_3$ on ZnO nanoparticles.

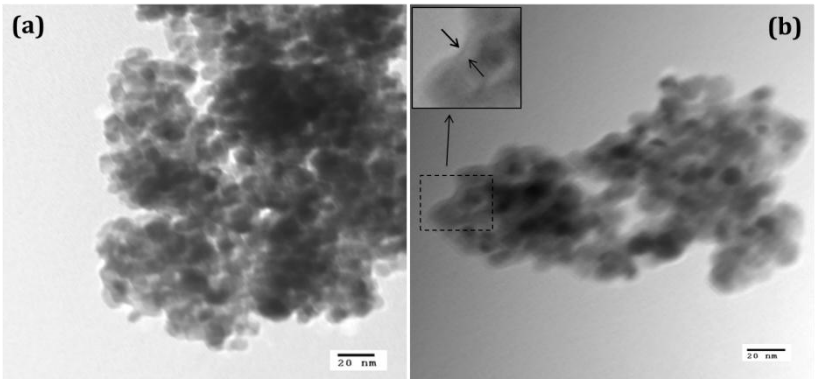


**Figure 3** TEM micrographs of (a) ZE0 and (b) ZE2 samples

**Dye desorption studies**

The fabricated photoelectrodes were immersed in 0.3mM ethanolic solution of N719 dye (20mL) for 20 hour. To desorb the dye molecules from the electrodes, they were soaked in 0.1mM aqueous NaOH solution. Figure 4 shows the UV-visible absorption spectra of the desorbed dye obtained from the electrodes. The peaks at 370 nm and 500 nm correspond to the characteristic absorption of N719 dye. The degree of dye adsorption on the electrode is proportional to the intensity of the optical absorption of dye. From the absorption study, it has

been found that the amount of dye adsorbed on the ZE1, ZE2 and ZE3 electrodes show enhanced dye adsorption as compared to the ZE0 electrode.

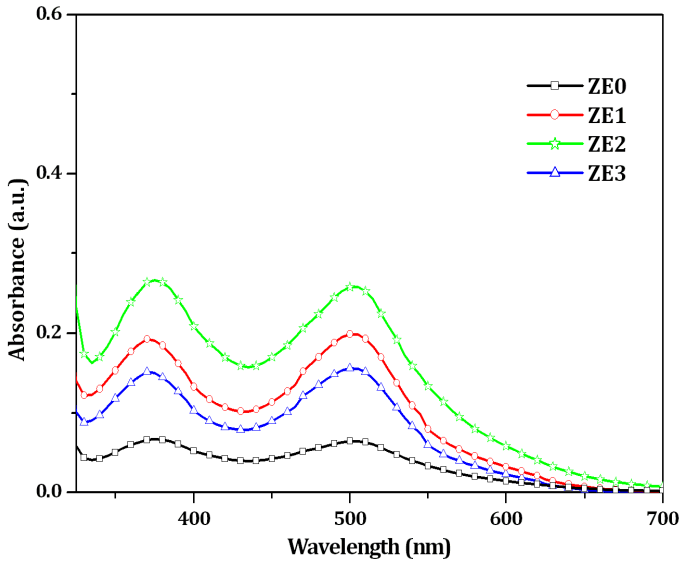


**Figure 4** UV–Vis absorption spectra of the N719 dye desorbed from (a) ZE0 (b) ZE1 (c) ZE2 and (d) ZE3 electrodes

The better adsorption of the dye molecules on $Eu_2O_3$/ZnO nanoparticles enhances the DSSC performance, as this increases the concentration of photogenerated electrons by visible light. The photocurrent of DSSC is influenced by the initial number of photogenerated electron-hole pairs, which depend on the film structure of the electrodes. The modification in film structure leads to the change in the light-harvesting capacity of photoelectrodes. Figure 4 illustrates that the electrode fabricated from the sample, ZE2 ensures maximum photon capturing in the visible region and furthermore indicates strong light-harvesting capacity. For the generation of high photocurrent density, the amount of dye adsorbed on nanocrystalline film should be high. The decrease in the adsorbed dye from ZE3 electrode is due to the decrease in the surface area of the working electrode due to high concentration of coating precursor.

**Photocurrent density-Voltage (J-V) characteristics:** Figure 5 shows the J-V curves obtained from DSSC fabricated using synthesized nanoparticles. Various parameters calculated from J-V curve are summarized in table 1, from which it can be seen that there is an increase in the short circuit current density ($J_{SC}$), open circuit voltage ($V_{OC}$), fill factor (FF) and efficiency (η) of DSSC fabricated from $Eu_2O_3$/ZnO nanoparticles compared to ZnO nanoparticles based DSSC. The coating $Eu_2O_3$ on ZnO acts as an energy barrier, which

minimizes the $e^-/h^+$ recombination and retards the back electron transfer to the electrolyte, resulting in increase in the value of open circuit voltage from 602 mV to 704 mV in case of ZE0 DSSC and ZE2 DSSC, respectively.

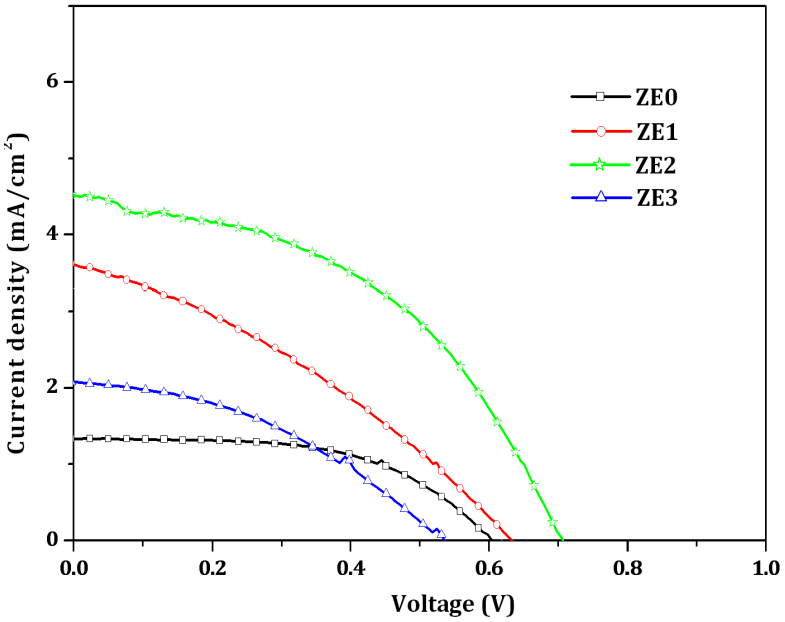


**Figure 5** J-V characteristics of DSSC fabricated using ZE0, ZE1, ZE2 and ZE3 samples

**Table 1** The different parameters of DSSC ($J_{SC}$, $V_{OC}$, FF and η), as calculated from the J-V characteristics

| Sample | $J_{SC}$ (mA/cm$^2$) | $V_{OC}$ (mV) | FF | η (%) |
|---|---|---|---|---|
| **ZE0** | 1.34 | 602 | 0.56 | 0.44 |
| **ZE1** | 3.61 | 630 | 0.33 | 0.77 |
| **ZE2** | 4.51 | 704 | 0.45 | 1.45 |
| **ZE3** | 2.06 | 536 | 0.38 | 0.43 |

An increase in the short circuit current density from 1.34 mA/cm$^2$ for ZE0 DSSC to 4.51 mA/cm$^2$ for ZE2 DSSC has been observed. The increase in short circuit current density can be explained by the fact that the amount of dye molecules adsorbed on $Eu_2O_3$/ZnO electrode is higher than the bare ZnO electrode.

## Synthesis and characterization of $Eu_2O_3$ coated $TiO_2$ nanoparticles and their application in dye sensitized solar cells

### Synthesis of $Eu_2O_3$ coated $TiO_2$ nanoparticles

Synthesis of $Eu_2O_3$ coated $TiO_2$ ($Eu_2O_3/TiO_2$) nanoparticles was done by a two-step process. For the coating of $Eu_2O_3$ on $TiO_2$ nanoparticles, 0.01M $EuCl_3$ in ethanol was reduced with $NaBH_4$, and, added in ethanolic solution of $TiO_2$ nanoparticles. Further, it was autoclaved for 14 hour at 150°C. The so obtained precipitates were filtered, washed and dried at 60°C for about 24 hour, and calcined at 500°C.

### Structural and phase analyses

To know the phase of $TiO_2$ nanoparticles and to validate the presence of $Eu_2O_3$ on $TiO_2$ nanoparticles, XRD analyses have been carried out. Figure 6 shows the XRD patterns of bare $TiO_2$ and $Eu_2O_3/TiO_2$ nanoparticles. XRD pattern of bare $TiO_2$ nanoparticles (figure 6(a)) reveals the formation of anatase phase with body-centered tetragonal structure (JCPDS Card No. 841286). In case of $Eu_2O_3/TiO_2$ nanoparticles, some additional peaks related to the body-centered structure of $Eu_2O_3$ (marked as E, figure 6(b)) have been observed (JCPDS Card No. 760154) along with anatase phase of $TiO_2$ (marked as T). These additional peaks corresponding to the cubic phase of $Eu_2O_3$ validate the presence of $Eu_2O_3$ on the surface of $TiO_2$.

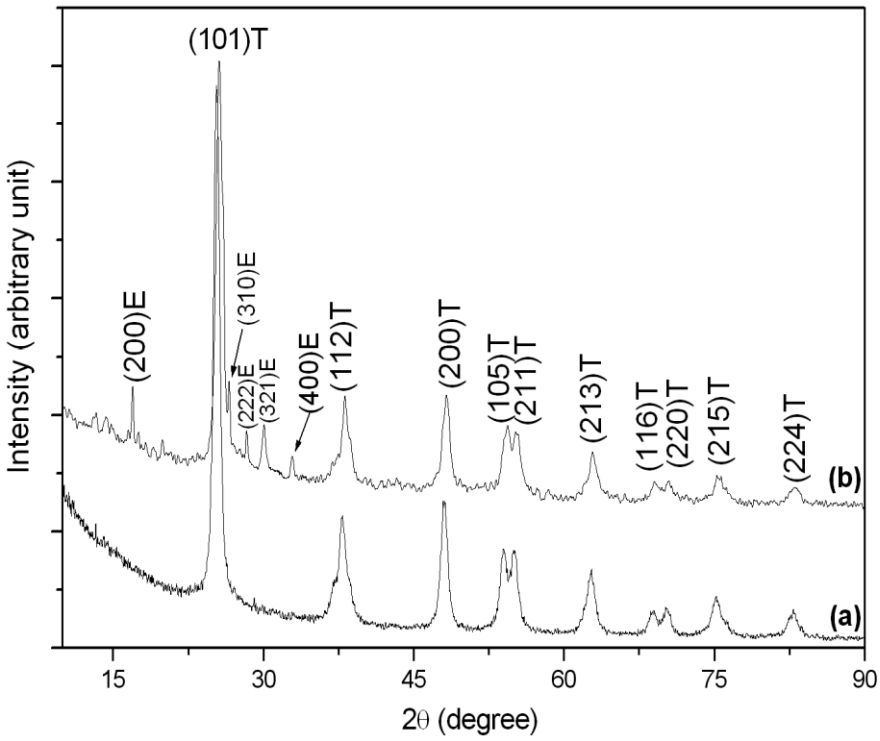


**Figure 6** X-ray diffractogram of (a) $TiO_2$ nanoparticles (b) $Eu_2O_3/TiO_2$ nanoparticles

Table 2 shows the crystallite size (D) of the nanoparticles as calculated from the XRD patterns, using Debye-Scherrer formula (eq. 1)

$$D = \frac{0.89\lambda}{\beta \cos\theta} \qquad (1)$$

where λ is the wavelength (λ = 1.54 Å), β is the full width at half maxima of the (101) peak, and θ is the corresponding diffraction angle.

**Table 2** Crystallite size calculated from the XRD pattern using Debye-Scherrer formula

| Sample | FWHM | 2θ | D (nm) | Phase |
|---|---|---|---|---|
| $TiO_2$ | 0.61 | 25.32 | 13.14 | Anatase |
| $Eu_2O_3/TiO_2$ | 0.65 | 25.60 | 12.37 | Cubic/Anatase |

The crystallite size of the $Eu_2O_3/TiO_2$ nanoparticles has been found to be smaller than the

bare $TiO_2$ nanoparticles.

**Compositional analysis**

Further to corroborate the XRD results, EDAX analysis has been carried out. The distribution of the Ti, O and Eu elements on the electrode surface were evaluated by EDAX dot-mapping (figure 7). The green, red and blue colours, respectively, show the EDAX dot mapping profile of Ti, O and Eu. It is clear from the EDAX dot mapping spectrum that the surface of $TiO_2$ contains Eu and O, which supports and confirms the formation of $Eu_2O_3$ coating on the surface of $TiO_2$ nanoparticles, as observed in XRD patterns as well (figure 6). Moreover, the EDAX spectrum also confirms the homogeneous presence of $Eu_2O_3$ coating on the $TiO_2$ surface.

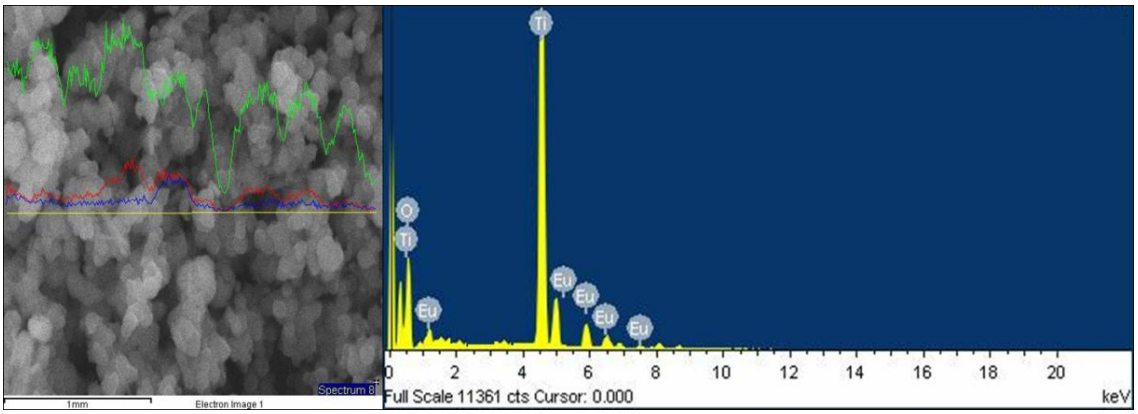


**Figure 7** EDAX dot maping spectrum of $Eu_2O_3/TiO_2$ nanoparticles

**Morphological study**

SEM micrographs of $TiO_2$ and $Eu_2O_3/TiO_2$ electrodes (figure 8(a) and 8(b)), show the formation of spherical nanoparticles, exhibiting porous nature. An increase in surface roughness is noticed in case of $Eu_2O_3/TiO_2$ (figure 8(b)) electrode, which leads to enhacement in the dye loading capability.

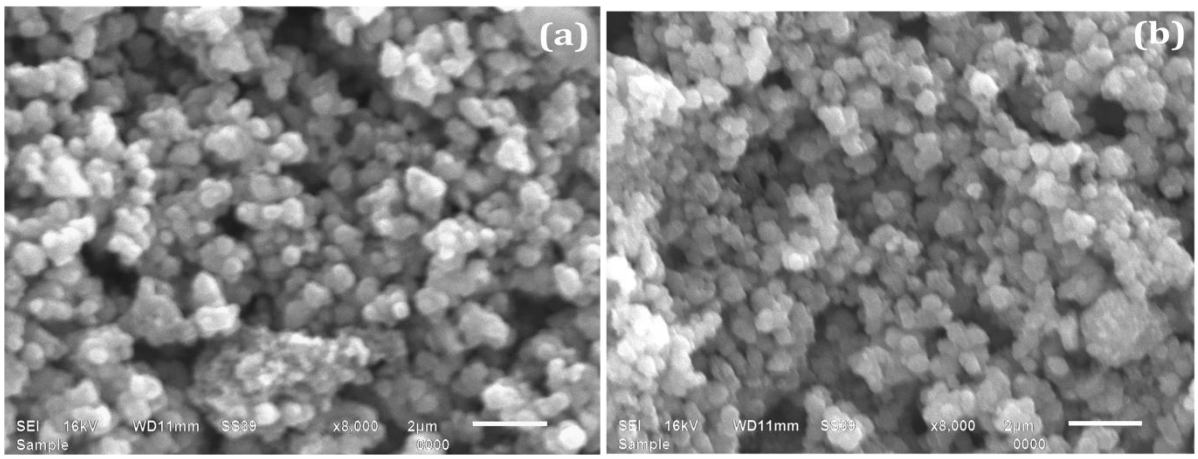


**Figure 8** SEM micrograph of (a) $TiO_2$ electrode, (b) $Eu_2O_3/TiO_2$ electrode

As it was difficult to distinguish $Eu_2O_3$ coating on the surface of $TiO_2$ nanoparticles from SEM analysis, hence the TEM study was carried out and micrographs are shown in figure 9(a) and 9(b), respectively, for $TiO_2$ and $Eu_2O_3/TiO_2$ nanoparticles.

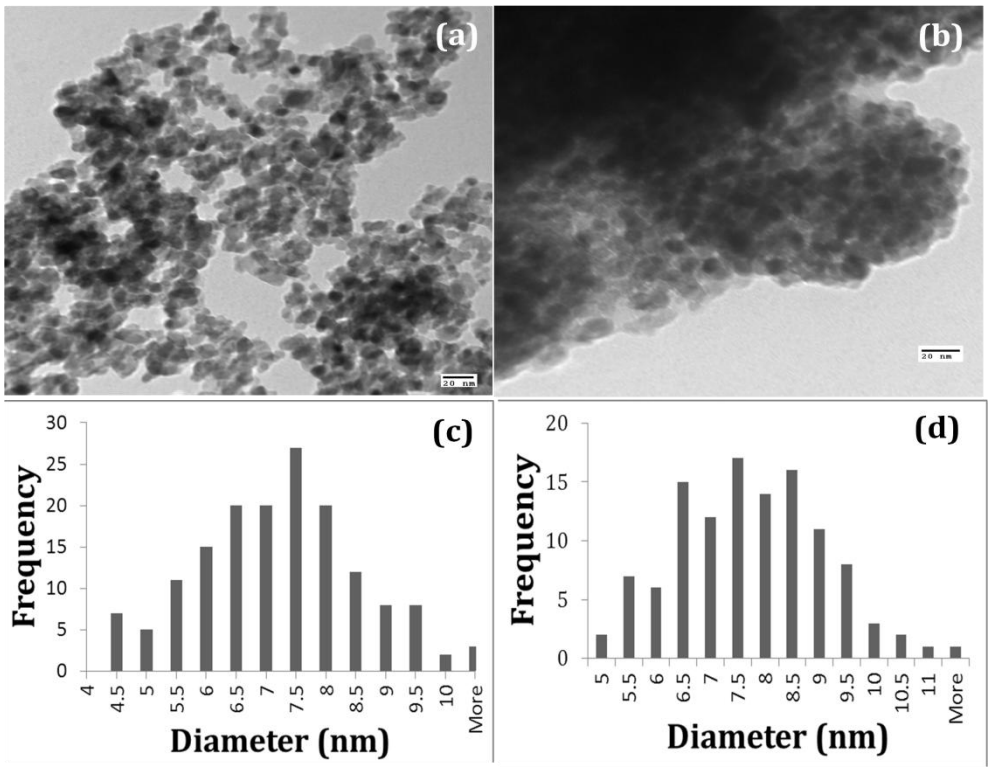


**Figure 9** TEM micrograph of (a) $TiO_2$, (b) $Eu_2O_3/TiO_2$ nanoparticles, Histogram of (c) $TiO_2$, (d) $Eu_2O_3/TiO_2$ nanoparticles

The narrow size distribution of the approximately equiaxed particles is well evident from the histogram in figure 4.4(c) and 4.4(d). The mean size of the bare $TiO_2$ and $Eu_2O_3/TiO_2$

nanoparticles has been found to be, respectively, 7 nm and 8 nm.

**Dye desorption study**

The $TiO_2$ and $Eu_2O_3/TiO_2$ photoelectrodes were immersed in 0.5mM ethanolic solution of N719 dye (20mL) for 20 hour. In order to compare the amount of dye adsorbed on the electrode fabricated using $TiO_2$ and $Eu_2O_3/TiO_2$ nanoparticles, UV-visible absorption study has been performed on the N719 dye desorbed from $TiO_2$ electrode and $Eu_2O_3/TiO_2$ electrode. The dyed film was dipped in 0.1 mM aqueous NaOH solution for 30 minute so that dye gets desorbed from the surface of the film. Figure 10 shows the UV-visible absorption spectra of N719 dye desorbed from both the films.

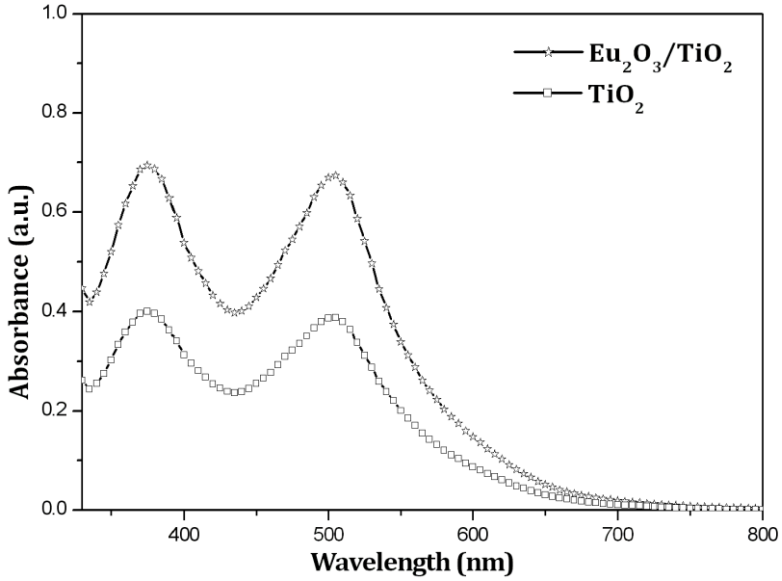


**Figure 10** UV–Vis absorption spectra of the N719 dye desorbed from $TiO_2$ electrode and $Eu_2O_3/TiO_2$ electrode

The better adsorption of the dye molecules on $Eu_2O_3/TiO_2$ nanoparticles is expected to enhance the DSSC performance, as the extent of dye adsorbed decides the concentration of photo-generated electrons by visible light. The absorbance of the desorbed dye from $Eu_2O_3/TiO_2$ nanoparticles film has been found to be 72% higher than that of bare $TiO_2$ nanoparticles, which makes the $Eu_2O_3/TiO_2$ nanoparticles a potential candidate for DSSC.

**Photocurrent density-Voltage (J-V) characteristics**

Figure 11 shows the typical J-V curves of the DSSCs fabricated using $TiO_2$ and $Eu_2O_3/TiO_2$ nanoparticles. J-V characteristics have been obtained by irradiating the assembled solar cells

with simulated solar light (100 mW $cm^{-2}$).

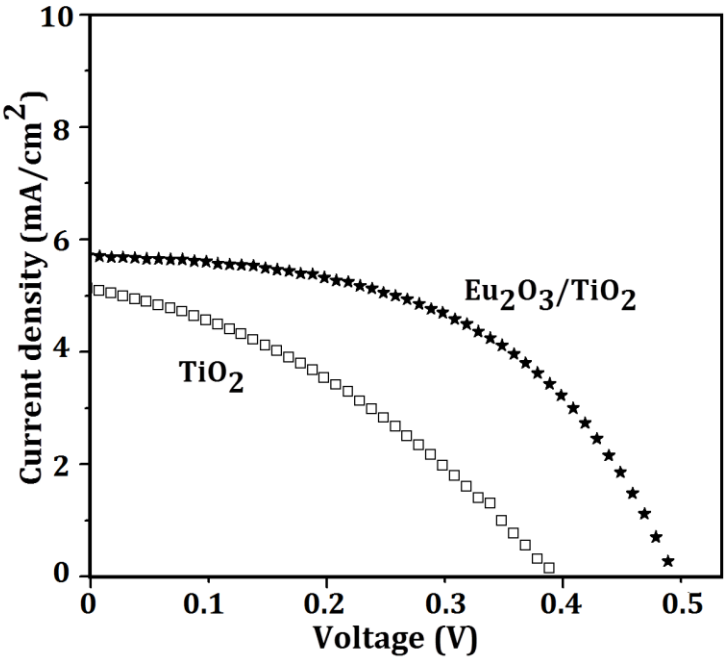


**Figure 11** J-V curves of $TiO_2$ and $Eu_2O_3/TiO_2$ dye sensitized solar cell

Table 3 summerizes the different parametrs short-circuit current density ($J_{SC}$), open circuit voltage ($V_{OC}$), fill factor (FF) and efficiency (η), as calculated from the J-V curves. An increase in $J_{SC}$, $V_{OC}$, FF and η has been observed in DSSC fabricated from $Eu_2O_3/TiO_2$ nanoparticles compared to $TiO_2$ nanoparticles.

**Table 3** Photovoltaic parameters as obtained from the J-V curve of DSSCs

| Sample | $J_{SC}$ (mA/$cm^2$) | $V_{OC}$ (V) | FF | η (%) |
|---|---|---|---|---|
| $TiO_2$ | 5.0 | 0.39 | 0.37 | 0.71 |
| $Eu_2O_3/TiO_2$ | 5.7 | 0.49 | 0.53 | 1.48 |

The increase in $J_{SC}$ can be explained by the fact that the amount of dye molecules adsorbed on $Eu_2O_3/TiO_2$ electrode is higher than the bare $TiO_2$ electrode as observed from dye desorbed studies (figure 10). The higher extent of absorption of dye molecules in case of $Eu_2O_3/TiO_2$ leads to higher $J_{SC}$, which results in greater light harvesting efficiency, and, hence, improves

the performance of DSSC. The coating of higher band gap $Eu_2O_3$ (4.1 eV) on $TiO_2$ acts as an energy barrier minimizing the electron-hole recombination by increasing the surface resistance of $TiO_2$ and retarding the back electron transfer to the electrolyte. Therefore, recombination rate decreases between the electrons in the conduction band of $TiO_2$ and the oxidized dye molecules at the surface of working electrode, which enhances the value of $V_{OC}$ from 0.39 V to 0.49 V. Moreover, the coating of $Eu_2O_3$ layer on $TiO_2$ surface lowers the electron loss between the FTO/electrolyte interface, which results in increasing the fill factor from 0.37 to 0.53. The efficiency of the DSSCs has been calculated using (eq. 2)

$$\eta = \frac{J_{SC} \times V_{OC} \times FF}{P_{in}} \qquad (2)$$

where $P_{in}$ is the power of the input light. The efficiencies have been found to be 0.71% and 1.48% for $TiO_2$ and $Eu_2O_3/TiO_2$ nanoparticles based DSSC, respectively. Similar results have been observed using coating of higher band gap material such as $SnO_2$, $CaCO_3$ on $TiO_2$ nanoparticles by various researchers. The enhancement of the cell parameters ($V_{OC}$, $J_{SC}$, FF) lead to an increase in the overall DSSC efficiency.

## Synthesis and characterization of $Tb_2O_3$ coated $TiO_2$ nanoparticles and their application in dye sensitized solar cells

### Synthesis of $Tb_2O_3/TiO_2$ nanoparticles

Synthesis of $Tb_2O_3/TiO_2$ nanoparticles was done by sol-gel and solvothermal method. First, $TiO_2$ nanoparticles were synthesized by sol gel method: the mixture of titanium isopropoxide and isopropyl alcohol was added drop-wise in a solution of water and isopropyl alcohol. The above solution was stirred for 5 h. The precipitates were collected, filtered, washed several times with water and ethanol; it was then dried at 65 ºC for about 24 h, and were further calcined at 450 ºC to obtain anatase phase $TiO_2$ nanoparticles.

For $Tb_2O_3$ coating, the synthesized $TiO_2$ nanoparticles were ultrasonically dispersed in ethanol, and in another beaker, 0.001 M $Tb(NO)_3)_3.5H_2O$ in ethanol was reduced with $NaBH_4$; it was magnetically stirred for 30 minutes. Now, this solution was added drop-wise to the dispersed $TiO_2$ nanoparticles and then stirred for 10 minutes to ensure homogeneous mixing. In this method, the primarily synthesized $TiO_2$ nanoparticles act as nucleation sites for the $Tb_2O_3$ coating. To allow the coating to uniformly form on the particles, and prevent the coating material from being produced separately from the particles, the coating solution

was added drop-wise. Further, the above mixture was transferred to Teflon container and autoclaved for 12 hour at 140ºC. The particles were washed and filtered. The particles thus obtained were calcined at 500ºC for 60 minute, to obtain crystalline nanoparticles (this sample is named as TiTb1). Similarly, two more samples were synthesized by adjusting the concentration of $Tb(NO)_3)_3.5H_2O$ to 0.005 M and 0.01 M (TiTb5 and TiTb10). For the fabrication of DSSC, doctor-blade technique was employed.

**Procedure for dye desorption**

The influence of $Tb_2O_3$ coating on dye adsorption has been investigated by measuring the absorption spectra of the N719 dye desorbed from the fabricated electrodes. To desorb the dye molecules from the electrodes, they were soaked in 0.1 mM aqueous NaOH solution.

**Structural and phase analysis**

Figure 12 shows the XRD spectra obtained from $TiO_2$, TiTb1, TiTb5 and TiTb10 samples. All the diffraction peaks match well with anatase structured $TiO_2$ with tetragonal phase (JCPDS File no. 84-1286). The peak positions of $Tb_2O_3/TiO_2$ were same as that of pure $TiO_2$. The crystallite size (D) has been calculated using the Debye Scherrer's formula

$$D = \frac{0.89\lambda}{\beta \cos\theta}$$

where λ is the wavelength (λ = 1.54 Å), β is the full width at half maxima of the (101) peak, and θ is the corresponding diffraction angle. Table 4 shows the crystallite size obtained from the Scherrer's formula for all the samples.

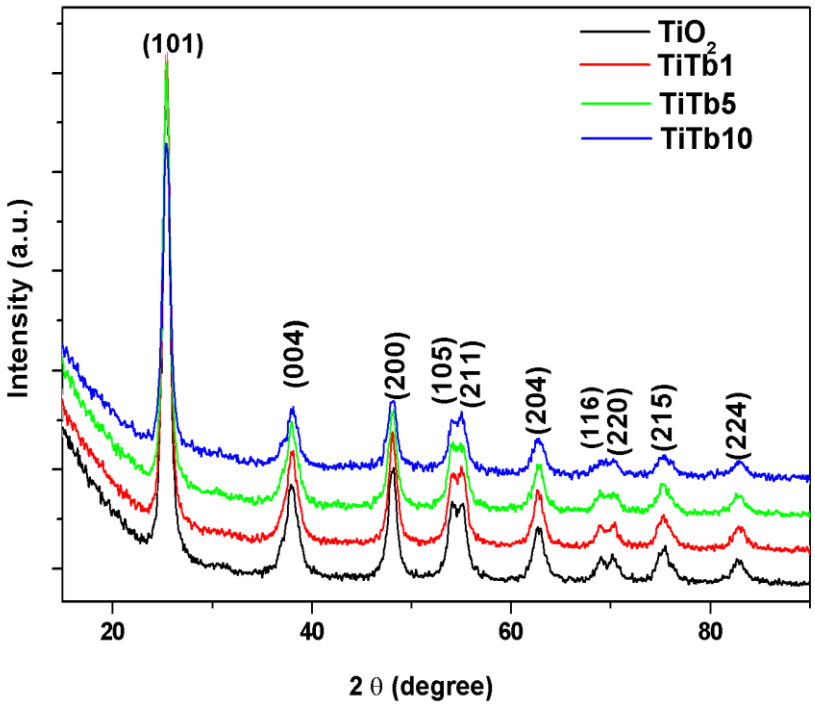


**Fig. 12** X-ray diffraction patterns of $TiO_2$, TiTb1, TiTb5, and TiTb10

**Table 1:** Crystallite size calculated from the XRD pattern using Debye–Scherer formula

| Sample | FWHM | 2θ | D (nm) |
|---|---|---|---|
| $TiO_2$ | 0.84 | 25.37 | 9.65 |
| TiTb1 | 0.80 | 25.39 | 10.11 |
| TiTb5 | 0.80 | 25.38 | 10.12 |
| TiTb10 | 0.86 | 25.39 | 9.46 |

The crystallite size calculated using Scherrer's equation has been found to be about 9.65, 10.11, 10.12 and 9.46 nm for $TiO_2$, TiTb1, TiTb5 and TiTb10 respectively. The data obtained from the Scherer's equation shows a slight increase in crystallite size with increase in $Tb_2O_3$ content. $Tb_2O_3$ coating influences the lattice structure and the crystallite size.

**Morphological analysis**

The presence of $Tb_2O_3$ on the surface of the $TiO_2$ nanoparticles has been established from TEM of TiTb1 sample. TEM micrographs of $TiO_2$ (Fig. 13(a)) and TiTb1 (Fig. 13(b)) nanoparticles are shown in figure 13. The average particle size of the bare $TiO_2$ and TiTb1 nanoparticles has been found to be, 9.3 nm and 10.1 nm, respectively, which reveal their

spherical nature. Figure 13 (b) confirms the coating (shown by dotted square in the inset) of $Tb_2O_3$ on $TiO_2$ nanoparticles.

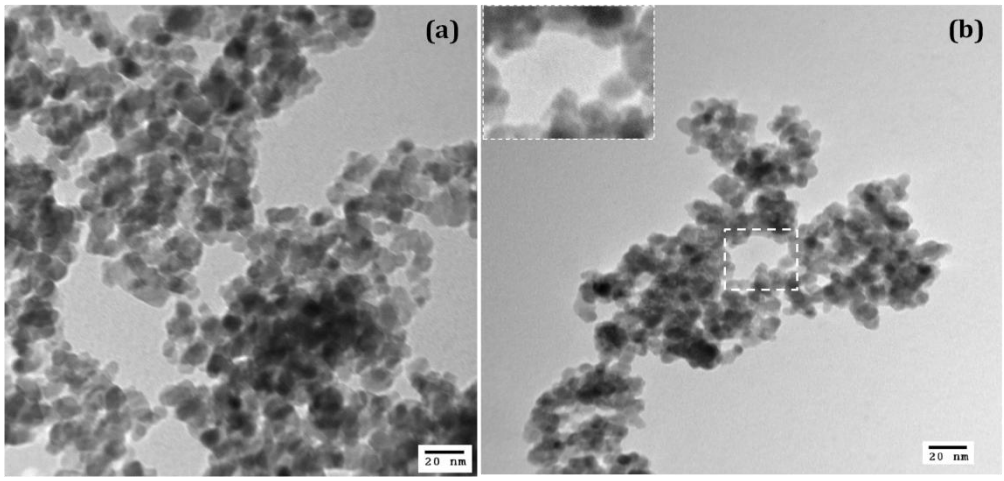


**Fig. 13:** TEM micrographs of (**a)** $TiO_2$ and (**b)** TiTb1 samples

**Compositional analysis**

Energy dispersive x-ray spectroscopy (EDAX) spectrum of TiTb1 sample has been shown in figure 14. The EDAX spectrum shows distinct peaks of O, Ti and Tb with atomic percentage 68.81, 30.62 and 0.57, respectively, concluding stoichiometric formation of TiTb1 sample. The analysis of EDAX spectrum concludes that the surface of $TiO_2$ contains Tb and O, which confirms the formation of $Tb_2O_3$ coating on the surface of $TiO_2$ nanoparticles.

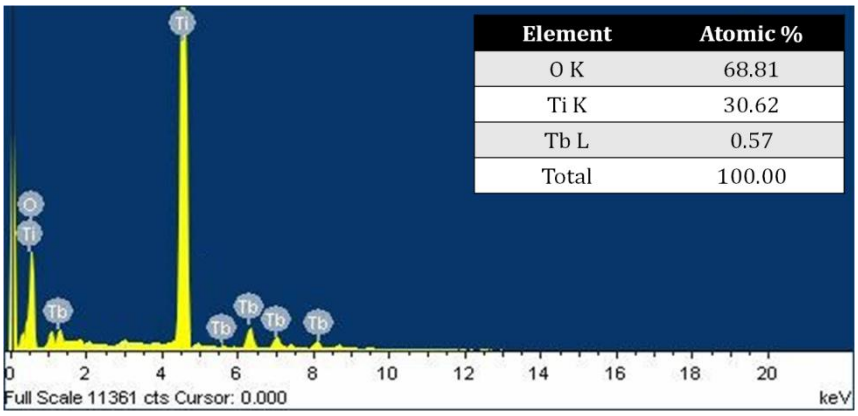


**Fig. 14:** EDAX spectrum of TiTb1 sample

**Dye desorption studies**

Figure 15 shows the UV–Visible absorption spectra of the N719 dye desorbed from the

electrodes. The peaks observed at 380 nm and 515 nm correspond to the characteristic absorption of N719 dye. The intensity of the UV-visible absorption is proportional to the degree of dye adsorption on the electrode. From the absorption study, it has been found that the amount of dye adsorbed on the TiTb1 electrode show enhanced dye adsorption as compared to the $TiO_2$ electrode.

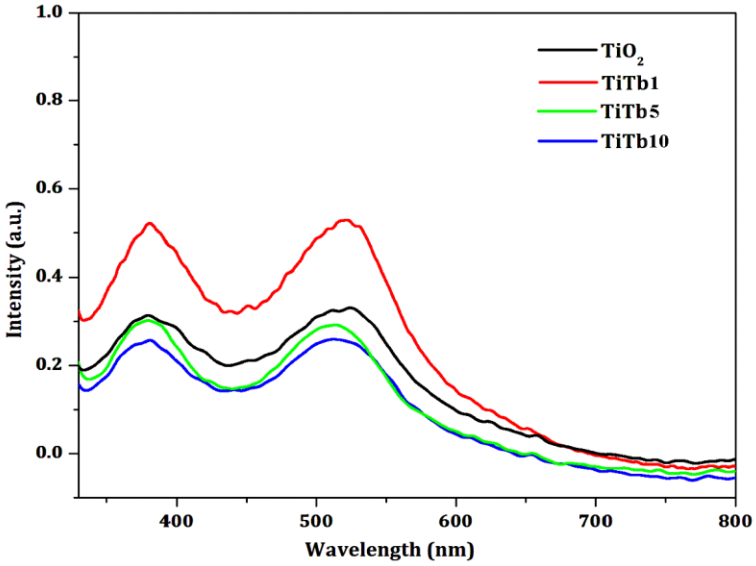


**Fig. 15:** UV–visible absorption spectra of the N719 dye desorbed from $TiO_2$, TiTb1, TiTb5 and TiTb10 electrode

The photocurrent of DSSC is influenced by the initial number of photo-generated electron–hole pairs, which depend on the film structure of the electrodes. Figure 15 illustrates that the electrode fabricated from TiTb1 sample shows maximum photon capturing in the visible region and furthermore indicate strong light-harvesting capacity. The enhanced adsorption of the dye molecules on TiTb1 based electrode, improves the DSSC performance as this increases the concentration of photo-generated electrons by visible light. For the generation of high photocurrent density, the amount of dye adsorbed on nanocrystalline film should be high. The decrease in the adsorbed dye from TiTb5 and TiTb10 electrodes is due to the decrease in the surface area of the working electrodes due to high concentration of coating precursor.

**Photocurrent density–voltage (J–V) characteristics**

Figure 16 shows the J–V curves obtained from DSSC fabricated using $TiO_2$, TiTb1, TiTb5 and TiTb10 nanoparticles, with an active area of 1 x 1 $cm^2$. The various parameters short

circuit current density ($J_{SC}$), open circuit voltage ($V_{OC}$), fill factor (FF) and efficiency (η) calculated from J–V curve are summarized in Table 5.

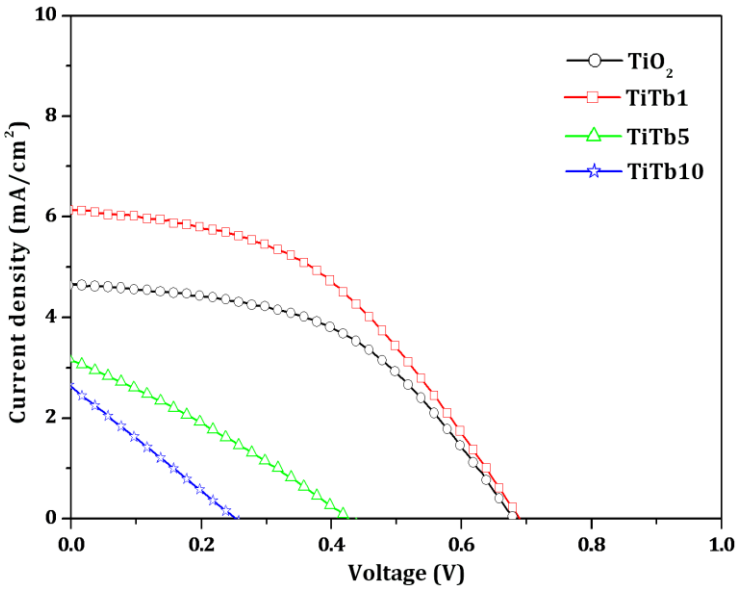


**Fig. 16:** J–V curves of $TiO_2$, TiTb1, TiTb5 and TiTb10 based DSSCs

An increase in the parameters has been registered in DSSC fabricated from TiTb1 nanoparticles compared to bare $TiO_2$ nanoparticles; this can be explained as under: the coating $Tb_2O_3$ on $TiO_2$ acts as an energy barrier, which minimizes the $e^-/h^+$ recombination and retards the back electron transfer to the electrolyte, resulting in increase in the value of open circuit voltage from 681 to 696 mV in case of $TiO_2$ DSSC and TiTb1 DSSC, respectively. The increase in Voc indicates the $Tb_2O_3$ coating on $TiO_2$ nanoparticles has decreased the recombination rate of the electron to the electrolyte.

**Table 5:** Photovoltaic parameters as obtained from the J–V curve

| Sample name | $J_{SC}$ (mA/cm$^2$) | $V_{OC}$ (mV) | FF | Efficiency (η) |
|---|---|---|---|---|
| $TiO_2$ | 4.66 | 681 | 0.48 | 1.54 |
| TiTb1 | 6.13 | 696 | 0.44 | 1.88 |
| TiTb5 | 3.16 | 421 | 0.29 | 0.38 |
| TiTb10 | 2.61 | 250 | 0.25 | 0.16 |

An increase in the short circuit current density, from 4.66 mA/cm$^2$ for $TiO_2$ DSSC to 6.13 mA/cm$^2$ for TiTb1 DSSC, has been observed. This increase in short circuit current density can be explained by the fact that the amount of dye molecules adsorbed on $Tb_2O_3/TiO_2$

electrode is higher than the bare $TiO_2$ electrode. The higher extent of absorption of dye molecules in case of $Tb_2O_3/TiO_2$ leads to higher $J_{SC}$, which results in greater light harvesting efficiency, and, hence, improves the performance of DSSC. The enhancement of $V_{OC}$ and $J_{SC}$ in the case of TiTb1 DSSC as compared to $TiO_2$ DSSC leads to an increase in the overall efficiency from 1.54% to 1.88%. However, TiTb5 and TiTb10 based DSSC show a decline in efficiency as compared to TiTb1 based DSSC. This is due to the fact that a thicker coating reduces the charge recombination more effectively, and, at the same time, it reduces the rate of electron injection into $TiO_2$. With increased $Tb_2O_3$ coating thickness, electron tunneling path increases and, as a result $J_{SC}$ decreases. The enhancement of the cell parameters ($V_{OC}$, $J_{SC}$, FF) lead to an increase in the overall DSSC efficiency.

**Papers published in refereed journals/conferences**

## Publications in SCI journals:

1. Manveen Kaur, N. K. Verma, 'Structural and optical properties of $Eu_2O_3$ coated $TiO_2$ nanoparticles and their application for dye sensitized solar cell', Journal of Materials Science: Materials in Electronics (2013) 24:1121–1127.
2. Manveen Kaur, N. K. Verma, 'Performance of $Eu_2O_3$ coated ZnO nanoparticles-based DSSC', Journal of Materials Science: Materials in Electronics, DOI 10.1007/s10854-013-1293-0 (2013).
3. Manveen Kaur, N. K. Verma, 'Performance of dye-sensitized solar cell fabricated using titania nanoparticles calcined at different temperatures', Materials Science-Poland, DOI: 10.2478/s13536-013-0114-8 (2013).

## Publications in non-SCI journals

1. Manveen Kaur, N. K. Verma, 'Application of $Eu_2O_3$/ZnO nanoparticles in dye sensitized solar cell', AIP Conference Proceeding, (2013) 1536: 69-70.
2. Manveen Kaur, N. K. Verma, '$Eu_2O_3$/ZnO nanocomposites for dye sensitized solar cell', Excel India Publishers, (2013) 2171-2176.

## Papers published in conferences:

1. Manveen Kaur, N. K. Verma, 'Synthesis and characterization of $Eu_2O_3$ coated ZnO nanoparticles', 23rd Annual General Meeting of Materials Research Society of India (MRSI), February 13-15, 2012, Thapar University, Patiala, pp. 88-89.

2. Manveen Kaur, N. K. Verma, Size and phase dependent performance of $TiO_2$ nanoparticles based dye sensitized solar cells, Emerging Trends in Physics for Environmental Monitoring & Management (ETPEMM-12), 17-19, December 2012, Punjabi University, Patiala, pp-33.
3. Manveen Kaur, N. K. Verma, Application Of $TiO_2$ Nanocubes In Dye Sensitized Solar Cell, International Conference on "Nanotechnology in the Service of Health, Environment and Society", 13-15 Feb (2014).
4. Manveen Kaur and N.K. Verma, "Synthesis and characterization of $Eu_2O_3$ coated $TiO_2$ nanoparticles" Proceedings of The National Conference on Nanoscience Fundamentals & Applications, July 23-24, 2011, pp 38.
5. Manveen Kaur and N.K. Verma, "Photocatalytic degradation of N719 dye by $TiO_2$ nanoparticles", Proceedings of 4th Bangalore Nano Conference, December 8-9, 2011, pp 107.